Recent experiments in neutron scattering by simple fluids

1996 J. Phys.: Condens. Matter 8 9111

(http://iopscience.iop.org/0953-8984/8/47/003)

J. Phys.: Condens. Matter **8** (1996) 9111–9126. Printed in the UK

Recent experiments in neutron scattering by simple fluids

F Barocchi†‡, U Bafile§ and R Magli‡‖

† Dipartimento di Fisica dell'Università, largo E Fermi 2, I 50125 Firenze, Italy
‡ Istituto Nazionale di Fisica della Materia, Sezione di Firenze, largo E Fermi 2, I 50125 Firenze, Italy
§ Istituto di Elettronica Quantistica, CNR, Via Panciatichi 56/30, I 50127 Firenze, Italy
‖ Dipartimento di Energetica "S. Stecco" dell'Università, via di S Marta 3, I 50139, Firenze, Italy

Received 13 August 1996

Abstract. Recent precise experimental results of neutron elastic and inelastic scattering in simple fluids, like noble gases in various density ranges, are briefly summarized. The comparison of these results with available theoretical calculations and the relevance of this experimental method, with the present state of the art, for the study of the microscopic properties of these systems are discussed.

1. Introduction

The study of the microscopic properties and of their connection with macroscopic properties of simple fluids made of closed-electronic-shell atoms, like noble gases, is of interest not only in itself but also because these systems are models which can be studied in detail with a good starting knowledge of the pair atomic interaction. Neutron elastic and inelastic scattering is one of the most interesting experimental tools for the determination of the microscopic structure and dynamics of fluids and it has been applied for a long time, especially to dense fluids like liquids [1, 2].

However, in the case of the structural studies, which are usually performed by deriving the static structure factor $S(k)$ from the experimental angular distribution of the neutron diffraction cross section, it has been thought that only minor details of the $S(k)$ are connected to the attractive microscopic interaction mechanism in the fluid while the excluded-volume effect induced by the step-like nature of the repulsive potential dominates [1]. This fact, therefore, if true to a high degree of accuracy, would lead to a good representation of real $S(k)$ even with hard-sphere-model potentials, despite the fact that the attractive part of the microscopic interaction certainly plays a role in determining the properties of the fluid.

Nevertheless, refined models for the pair interaction of closed-electronic-shell atoms, derived from various physical properties of single pairs, are available [3] and also the theory which connects the microscopic potential interaction with the structure, represented by the pair distribution function $g(r)$ in the fluid at any density, has been brought up to include the effect of the irreducible long-range three-body interaction [4]. Moreover, computer simulation methods are now able to investigate the behaviour of microscopic correlations, both static and dynamic, in a very large number of thermodynamic states and in a very large (k, ω) domain, giving the possibility of performing calculations with model potentials to compare with experimental results.

0953-8984/96/479111+16$19.50

Present neutron scattering instrumentation and data analysis treatment have also reached a high level of accuracy for the structural experiments and new inelastic instruments of high resolution are now available. Therefore it seems to be right to undertake a systematic study of the connection between the microscopic interaction in simple systems and the structural and dynamical properties in order to establish this connection at the level of the present state of the art for theory and neutron scattering experiments.

Here we will briefly report on a series of recent experiments, performed in noble gases both for structural and for dynamical studies, and on the comparison of the experimental results with available theories, in order to clarify the current possibilities. We consider the present state of the art for the determination of the static structure factor $S(k)$ in simple fluids, measurements of $S(k)$ with an absolute precision of the order of 0.5% and a relative statistical accuracy in the range 0.1–0.01%, whereas the best accuracy for the dynamical structure factor $S(k, \omega)$ is of the order of few per cent. We will discuss (i) the static structure factor $S(k)$ at low density as determined by normal diffraction, (ii) the small-k behaviour of $S(k)$ at low density, (iii) the static structure factor in dense fluids, (iv) the low-density $S(k, \omega)$ at small angles and (v) the small angle $S(k, \omega)$ in moderately dense gases. Let us first give some theoretical background for the structural and dynamic properties.

2. Structural properties

In the theory of simple fluids, the static structure factor $S(k)$ and the Fourier transform $c(k)$ of the direct correlation function $c(r)$ are defined by [1]

$$S(k) = 1 + n \int \mathrm{d}\boldsymbol{r} \exp(-\mathrm{i}\boldsymbol{k} \cdot \boldsymbol{r})(g(r) - 1) \tag{1}$$

$$c(k) = \int \mathrm{d}\boldsymbol{r} \exp(-\mathrm{i}\boldsymbol{k} \cdot \boldsymbol{r})c(r) \tag{2}$$

where $g(r)$ is the pair correlation function and $c(r)$ is given by the Ornstein–Zernike relation

$$h(r) = c(r) + n \int \mathrm{d}\boldsymbol{r}' c(r')h(|\boldsymbol{r} - \boldsymbol{r}'|) \tag{3}$$

with

$$h(r) = g(r) - 1. \tag{4}$$

$S(k)$ is the experimentally accessible quantity and $c(k)$ can be derived from $S(k)$ by using the relation

$$c(k) = (S(k) - 1)/nS(k) \tag{5}$$

obtained from equations (1)–(4). $c(r)$ and consequently $c(k)$ have an important role in the theory of fluids and are a useful representation of correlations because they reflect the properties of the interatomic interaction at intermediate and large distances more directly than does $g(r)$.

Here we will consider only classical systems. The $g(r)$ and $c(r)$ are functionals of the interatomic interaction $U(\boldsymbol{r}_1, \ldots, \boldsymbol{r}_N)$ which we will assume to be represented by the cluster expansion

$$U(\boldsymbol{r}_1, \ldots, \boldsymbol{r}_N) = \sum_{i<j} U_2(r_{ij}) + \sum_{i<j<l} U_3(\boldsymbol{r}_i, \boldsymbol{r}_j, \boldsymbol{r}_l) \tag{6}$$

where $\boldsymbol{r}_i$ is the position of the ith atom, $r_{ij} = |\boldsymbol{r}_j - \boldsymbol{r}_i|$ and we have neglected many-body forces beyond the triplet level. Here U_2 and U_3 are the pair and triplet irreducible interaction potentials respectively.

In the low-density limit $c(r)$ and $c(k)$ can be given as series expansions with respect to the density n of the system so that

$$c(r) = c_0(r) + nc_1(r) + O(n^2) \tag{7}$$

$$c(k) = c_0(k) + nc_1(k) + O(n^2) \tag{8}$$

where for $j = 0, 1$

$$c_j(k) = \int \mathrm{d}\boldsymbol{r} \exp(-\mathrm{i}\boldsymbol{k} \cdot \boldsymbol{r}) c_j(r) \tag{9}$$

$$c_j(r) = (2\pi)^{-3} \int \mathrm{d}\boldsymbol{r} \exp(\mathrm{i}\boldsymbol{k} \cdot \boldsymbol{r}) c_j(k). \tag{10}$$

It is easy to show that, for classical fluids,

$$c_0(r) = \exp(-\beta U_2(r)) - 1 \tag{11}$$

where $\beta = 1/(k_B T)$ and T is the temperature of the system. Moreover $c_1(r)$ is the term which accounts for the three-body correlations, namely for the first deviation of $c(r)$ from pure pair behaviour [5, 6].

From equation (9) it is immediately seen that

$$U_2(r) = -K_B T \ln(c_0(r) + 1). \tag{12}$$

Therefore, from a measurement of $c_0(k)$ over a wide range of k values and by means of equations (9) and (11) one can derive an experimental pair potential for the system under consideration.

It is interesting also to discuss the long-range behaviour of $c(r)$ in connection with the small-k behaviour of the $c(k)$. In fluid systems the interaction law can be written retaining only the pair and the triplet contributions, equation (6), and it has been demonstrated that, under these conditions the asymptotic behaviour of $c(r)$, under approximating assumptions within the MHNC theory, is given by [7]

$$c(r) \simeq -\beta U_2(r) + C(r) \qquad \text{for } r \to \infty \tag{13}$$

where $C(r)$ is the dressed three-particle vertex. When the dispersion term is the dominant one in the long-range pair potential we have

$$U_2(r)_{r\to\infty} \simeq -C_6/r^6. \tag{14}$$

Moreover, if the irreducible three-body interaction is assumed to be of the triple-dipole Axilrod–Teller (AT) form [8] it can be demonstrated [9, 7] that we can write

$$C(r)_{r\to\infty} \simeq -(8\pi/3)\beta n \nu / r^6. \tag{15}$$

Here ν is the strength of the AT potential.

By using expressions (12)–(14) and asymptotic Fourier analysis it can be shown that the small-k expansion of $c(k)$ is given by [10, 7]

$$c(k)_{k\to 0} \simeq c(0) + c_2 k^2 + c_3 |k|^3 \tag{16}$$

where the $|k|^3$ term is due to the r^{-6} two- and three-body potential tails in direct space and the c_3 coefficient is given by

$$c_3 = (\pi^2/12)[C_6 - 8\pi n \nu/3] k_B T. \tag{17}$$

The previous expression indicates that, if a linear density-dependence at small densities is found in c_3 this demonstrates that the Axilrod–Teller potential can be correct, while, together with C_6, a measure of the ν coefficient can be extracted from the density-dependence.

In the case of dense systems the theory is performed by means of integral equations, the most refined one is the triplet MHNC, which encloses the effect of the three-body potential [4]. The fundamental relation between correlations and interactions for the triplet MHNC is the expression

$$g(r) = \exp(-\beta U_2(r) + h(r) - c(r) + C(r) + E_{HS}(r)) \tag{18}$$

where $C(r)$ is the dressed three-particle vertex and $E_{HS}(r)$ is the hard-sphere bridge function. We have also

$$C(r) = n \int \mathrm{d}\boldsymbol{r}_3 g(r_{13}) g(r_{23}) [\exp(-\beta U_3(\boldsymbol{r}_1, \boldsymbol{r}_2, \boldsymbol{r}_3)) - 1]. \tag{19}$$

Equations (3), (18) and (19) form a closed set of equations for $g(r)$, which enclose the effects of two- and three-body forces, and which can be solved with a suitable iterative method.

3. Dynamic properties

Differently from the case of structure, a detailed theory of dynamical properties in simple fluids does not exist up to now; nevertheless, several models have been employed in order to account for these properties in an approximate way and to compare experimental results with theoretical predictions. Here we will give two examples, one for low and one for high density, relevant for discussing the small-k behaviour of $S(k, \omega)$.

The density expansion of $S(k, \omega)$, similarly to the case of $S(k)$, can be usefully discussed if we restrict ourselves to considering (k, ω) ranges within which effects due to long-time tails in the correlation functions, from which $S(k, \omega)$ itself originates, are negligible within the experimental uncertainties [11, 12]. In this context we must avoid in our study the region in (k, ω) space within which collective modes are manifest in the spectrum of the density fluctuations in the system. For this purpose we consider that we must fulfil one of the two requirements $k \gg 1/l$ or $\omega \gg 1/\tau$ where l and τ are the mean free path and the free time between collision in the system respectively.

When one of the two previous conditions is fulfilled then, similarly to what it is done for $S(k)$, also $S(k, \omega)$ can be expanded in a series with respect to the density of the system as

$$S(k, \omega)/S(k) = S^{(0)}(k, \omega) + nS^{(1)}(k, \omega) + O(n^2) \tag{20}$$

where $S^{(0)}(k, \omega)$ is the free-gas contribution and equals the dynamic structure factor for non-interacting particles, while the linear term $nS^{(1)}(k, \omega)$ represents the contribution due to the interaction and dynamics of pairs. The higher order terms in equation (20) are negligible for $n\sigma^3 \ll 1$, where σ is the size of the particles.

Up to now the explicit calculation of $S^{(1)}(k, \omega)$ has been performed for a hard-sphere fluid only by Kamgar-Parsi *et al* [11]. These authors use an expansion equivalent to (20) at low density ($V_0/V < 0.1$ which is equivalent to $n\sigma^3 < 0.14$, where V_0 is the close-packing volume). This expansion is in powers of $1/(kl_0)$, where $l_1 = (n\pi\sigma^2\sqrt{2})^{-1}$ is the Boltzmann free path, and is given by

$$S(k, \omega)/S(k) = 2t_0/(\pi k l_0)[\exp(-4\omega^{*2}/\pi) + s_{11}(\omega^*)/(kl_0) + O(kl_0)^{-2}] \tag{21}$$

where $t_0 = l_0[\pi M/(8k_B T)]^{1/2}$ is the Boltzmann mean free time and M is the particle mass. In this last expression the frequency-dependence appears only through the reduced variable

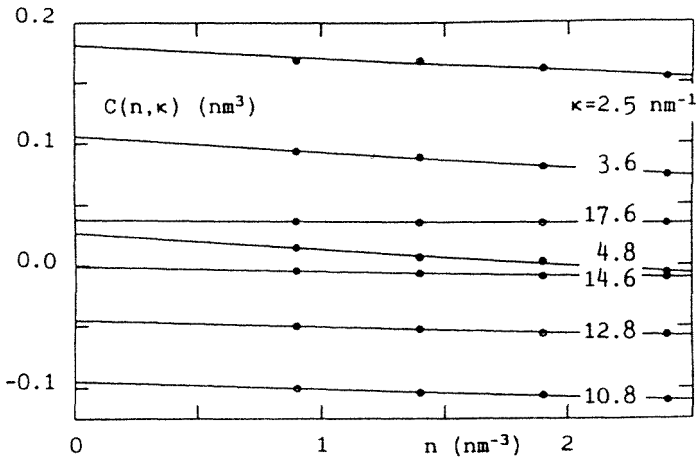

Figure 1. Experimental $c(k, n)$ at various k values (symbols) and weighted linear fits to the data (lines).

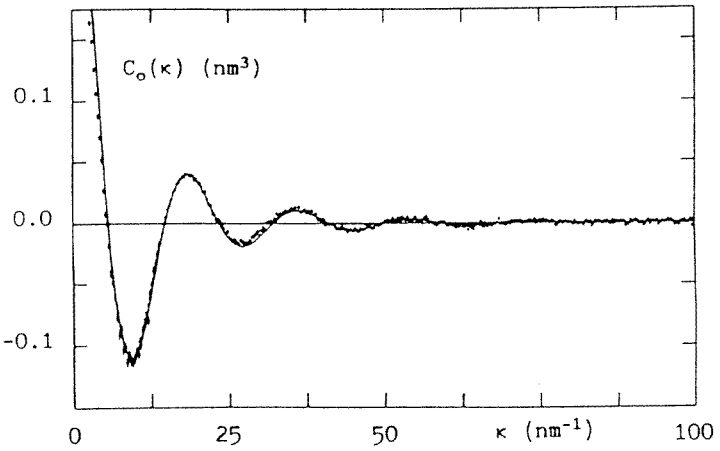

Figure 2. $c_0(k)$ from extrapolation of $c(k, n)$ to $n = 0$ (symbols) and calculated from the pair potential taken from [15] (line).

$\omega^* = \omega t_0/(kl_0)$. The first term in equation (21) is again the free-gas contribution, while $s_{11}(\omega^*)$ is related to $S^{(1)}(k, \omega)$ for hard spheres by

$$s_{11}(\omega^*) = [k_B T/(\pi M)]^{1/2}(k/\sigma)^2 S^{(1)}(k, \omega). \tag{22}$$

At higher density linearized hydrodynamics can be used to interpret the experimental $S(k, \omega)$ in the (k, ω) region within which collective modes are manifest in the spectrum of the density fluctuations in the system.

In this case we can write $S(k, \omega)$ as a sum of three Lorentzians [13], namely

$$S(k, \omega) = (S(k)/\pi)\{A_0 z_H/(\omega^2 + z_H^2)\} + A_S[z_S + (\omega + \omega_S)b]/[(\omega + \omega_S)^2 + z_S^2] + A_S[z_S - (\omega - \omega_S)b]/[(\omega - \omega_S)^2 + z_S^2] \tag{23}$$

where the quantities $A_0, A_S, z_H, z_S, \omega_S$ and b can be given in terms of the specific heat

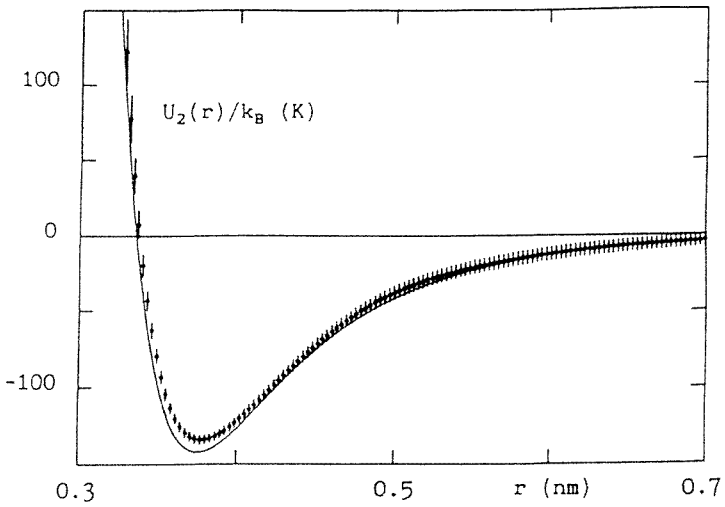

Figure 3. Pair potentials from experiment (symbols) and from the literature [15].

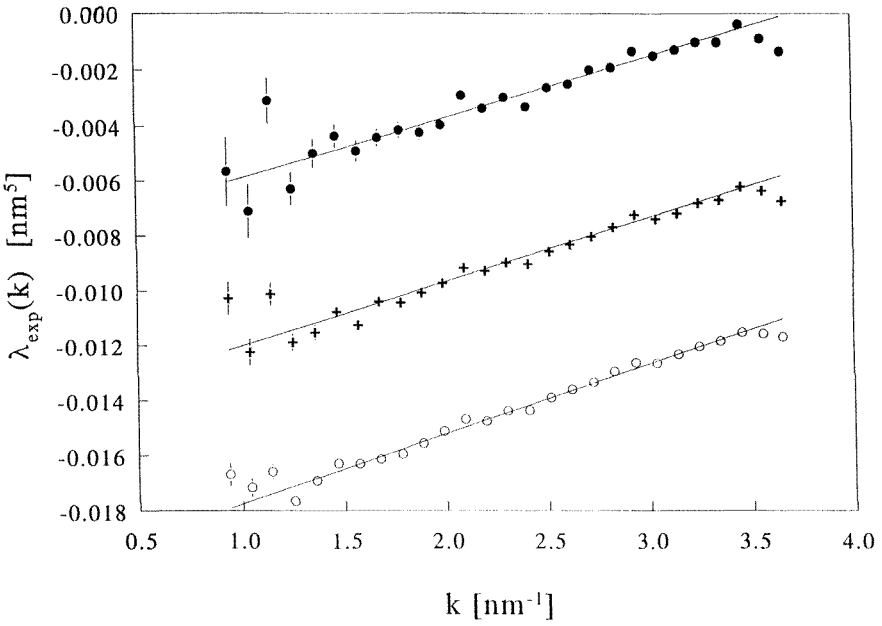

Figure 4. Experimental results for $\lambda(k)$ in argon at $T = 138.75$ K. The densities are, from top to bottom: $n = 1.51, 199$ and 2.30 nm^{-3}. The data for $n = 1.99$ and 1.51 nm^{-3} are shifted upward by 0.005 and 0.01 respectively. Straight lines represent the results of the fitting procedure.

ratio $\gamma = C_p/C_v$, the kinematic longitudinal viscosity $\nu = (\eta_b + \frac{4}{3}\eta_S)/(nM)$, η_S the shear viscosity, η_b the bulk viscosity, the thermal diffusivity $a = \lambda/(nC_p)$ and c_S the speed of sound. For low enough k such that γak^2 and νk^2 are small compared to $c_S k$ equation (23)

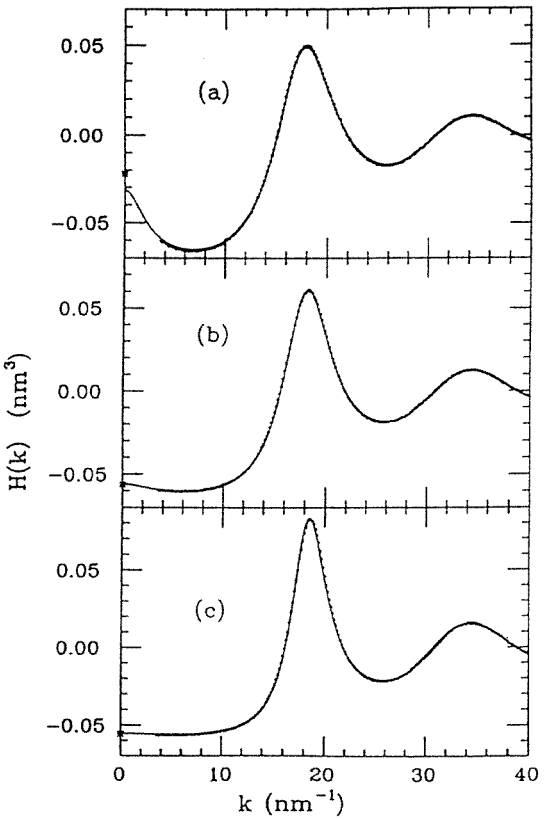

Figure 5. Details of the $H(k)$ for krypton in the small–intermediate-k range: (a) $T = 199$ K, $n = 11.86$ nm^{-3}; (b) $T = 169$ K, $n = 14.57$ nm^{-3}; and (c) $T = 130$ K, $n = 16.83$ nm^{-3}. The full curve is the result of the triplet MHNC equation with the Aziz pair interaction plus the three-body AT term. The values at $k = 0$ are taken from the compressibility data.

reduces to the well-known Rayleigh–Brillouin triplet with

$$A_0 = (\gamma - 1)/\gamma \qquad A_S = 1/(2\gamma) \qquad \omega_S = c_S k$$
$$z_H = ak^2 \qquad z_S = \Gamma k^2 \tag{24}$$

where $\Gamma = [\nu + (\gamma - 1)a]/2$ is the sound damping factor.

4. The static structure factor $S(k)$ at low density as determined by normal diffraction

From equations (7) and (10) it is clear that a precise measurement of the density behaviour of $c(k)$ and the consequent determination of the zero-density limit $c_0(k)$ give the possibility of evaluating, by means of a simple Fourier transformation, $c_0(r)$ and then by equation (12) of extracting an experimental pair potential. This is a possibility of direct experimental determination of the pair potential between two atoms by means of a simple Fourier transformation of diffraction data. The precision of this procedure depends on the accuracy of the determination of $c_0(k)$, but also very much on the range of k within which $c_0(k)$ is measured, the larger the range the higher the precision attainable for a given experimental accuracy.

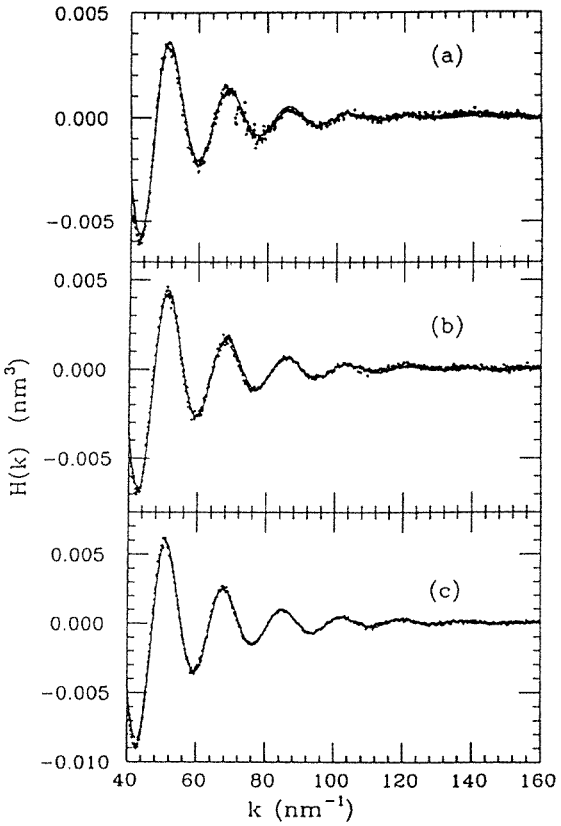

Figure 6. Details of $H(k)$ in the large-k range: (a), (b) and (c) are as in figure 5.

The first experiment for the determination of the pair potential from neutron diffraction measurements was performed in argon [14] with the diffractometer D4B at the ILL in Grenoble. Figure 1 shows an example of the density behaviour of $c(k)$ at various k values for argon, at low density and temperature $T = 140$ K, from which the linear density-dependence of equation (8) is demonstrated. From this density behaviour the $c_0(k)$ is then extracted in the k range $2.4 < k < 100$ nm^{-1}. Figure 2 shows the experimental $c_0(k)$ of argon at $T = 140$ K. From Fourier transformation of $c_0(k)$ we can now determine $c_0(r)$ and $U_2(r)$ using equation (12). Figure 3 shows the experimental potential extracted from the data and compared with a model potential for argon given in [15]. The comparison is good and demonstrates the power of the method, even though it is not completely satisfactory. Part of the difference may be attributed to the lack of data at lower k values and the consequent impossibility of using also the $k = 0$ limit of $c_0(k)$ which can be precisely derived from PVT data.

5. The small-k behaviour of $c(k)$ at low density

In order to measure the small-k dependence of $c(k)$ at low density given by equation (16) an experiment was performed on argon gas with the PAXE SANS diffractometer at the LLB, Saclay [16]. From this experiment the $|k|^3$ behaviour of $c(k)$ at low k was determined and

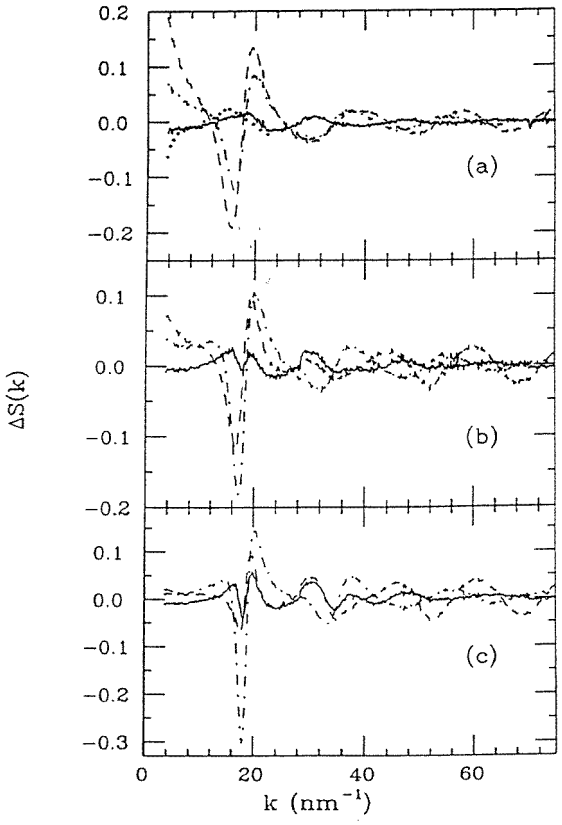

Figure 7. The difference $\Delta S(k)$ for the Aziz pair interaction with the AT three-body potential (full curve), for the LJ interaction (chain curve) and for the hard-sphere potential (broken curve). The result for the Aziz interaction without the three-body term (points) is only shown in (a) up to 20 nm^{-1}. Thermodynamic states are as in figure 5.

the first measurement of the coefficient C_6 of the London dispersion interaction in the argon pair potential performed.

In order to display the $|k|^3$-dependence of the experimental $c_{exp}(k)$ it is more convenient to refer to the quantity $\lambda(k)$ defined by

$$\lambda(k) \underset{k\to 0}{=} (c(k) - c(0))/k^2 \sim c_2 + c_3 k. \tag{25}$$

Figure 4 shows the experimental results for argon at $T = 138.75$ K for three different densities; here the function is given by equation (16), where $c(0), c_2$ and c_3 are the coefficients derived from a least-squares fit performed on $c(k)$ with the polynomial (16). From figure 4 the k-dependence of $\lambda(k)$ and therefore the $|k|^3$-dependence of $c(k)$ is demonstrated. In this case no density-dependence of the experimental c_3 coefficient is found; in particular, from the experimental value of c_3, the value of C_6 for argon can be derived. This value is $C_6 = (5.54 \pm 0.83) \times 10^{-78}$ J m^6 and compares very well with the estimate given by Kumar and Meath [17], $C_6 = 6.16 \times 10^{-78}$ J m^6.

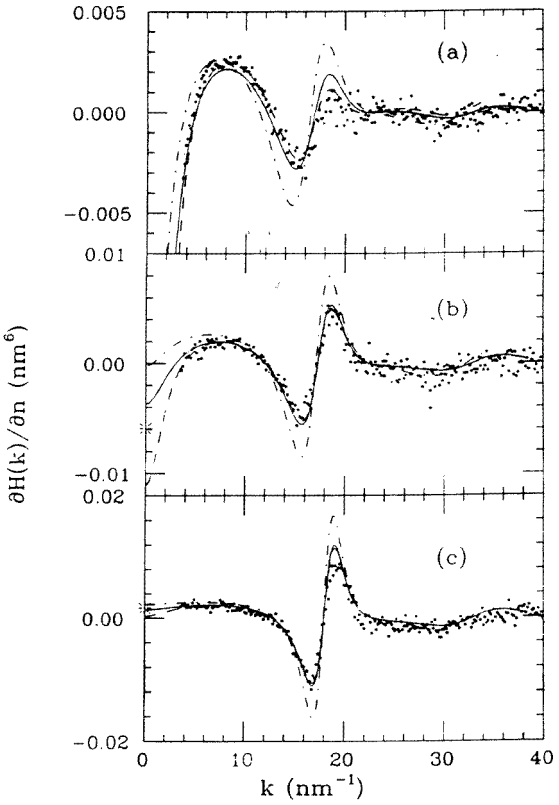

Figure 8. The density derivative of $H(k)$ for the Aziz pair interaction with (full curve) and without the AT three-body term (broken curve), for the LJ interaction (chain curve) and from experimental data (points). The thermodynamic states for (a), (b) and (c) are as in figure 5.

6. The static structure factor in dense fluids

We now turn to the discussion of some experimental results for the $S(k)$ at high density in krypton [18, 19]. These measurements were performed at several temperatures between the triple point and the critical point and at several different densities in order to compare precise experimental $S(k)$ with theoretical prediction. The theory to which we will refer, for normal conditions far from the critical point, is the result of calculations based on the three-body MHNC of equation (18) which gives $g(r)$ starting from a model potential for U_2 and U_3. These calculations were performed for three different pair potentials in order to distinguish among them, namely the hard-spheres (HS), the Lennard-Jones (LJ) and the empirical pair potential given in [20], for the three-body potential the Axilrod and Teller potential was used. Figures 5 and 6 give the comparison for $H(k)$ between the experimental results and the calculations with the empirical pair potential for three different thermodynamic states; here also the $k = 0$ compressibility limit is reported. $H(k)$ is defined as $H(k) = (S(k) - 1)/n$.

The very high degree of agreement is better seen in the quantity $\Delta S(k) = S_{exp}(k) - S_{MHNC}(k)$ defined as the difference between experiment and calculation. Figure 7 gives $\Delta S(k)$ for the various pair potentials with and without the three-body one.

Here it is shown that the result for the empirical Aziz potential is by far the best; in this

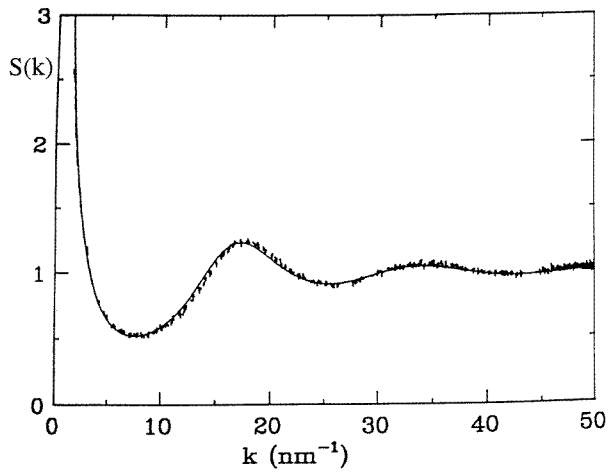

Figure 9. Experimental (dots) and theoretical (full line) $S(k)$ of Kr at $T^* = 4.4 \times 10^{-3}$ and $n = 7.25$ nm^{-3}.

case at the two highest temperatures $\Delta S(k)$ is of the order of 0.02 whereas at $T = 130$ K it is 0.05, only at $T = 199$ K does the introduction of the three-body interaction give a very slightly better agreement. At the two lower temperature and higher densities the effect of U_3 is appreciable only in the neighbourhood of $k = 0$. For the LJ potential $\Delta S(k)$ is typically 5–10 times larger than that for the empirical model potential and is particularly large in the region of the first maximum. As expected the hard-sphere $S(k)$ gives a rather good description at the higher density, whereas, as we move to lower density the deviations become significant throughout the k range.

Even more interesting is the comparison between theory and experiment for the density derivative of $S(k)$. For convenience we will refer here to the density derivative of $H(k)$. Figure 8 shows this derivative for three different thermodynamic states compared with theoretical calculations. On comparing figures 7 and 8, we notice that the difference between the two potentials in the case of the derivative is in the first peak region, ten times larger than for $S(k)$ itself, which makes the derivative more suitable for testing the potential form in dense systems.

Comparison between experiments and theory can also be performed in the vicinity of the critical point, namely for reduced temperatures $T^* = (T - T_c)/T_c$ of the order of 10^{-3}–10^{-2}. This is done by using an integral equation theory different from the MHNC, which is known not to converge near the critical point; this new theory, given in [21]. is the hierarchical reference theory (HRT).

Figure 9 shows the comparison of the experimental and theoretical $S(k)$ of krypton at $T^* = 4.4 \times 10^{-3}$ and density $n = 7.25$ nm^{-3}. The calculation is the result of the HRT with the Aziz potential. The agreement is quite good also in the small-k region where the critical divergence starts to show [22].

7. The low-density $S(k, \omega)$ at small angles

In order to study the deviations from the free-gas behaviour in the $S(k, \omega)$, as represented by equation (20), and the connection of these deviations with the microscopic interaction,

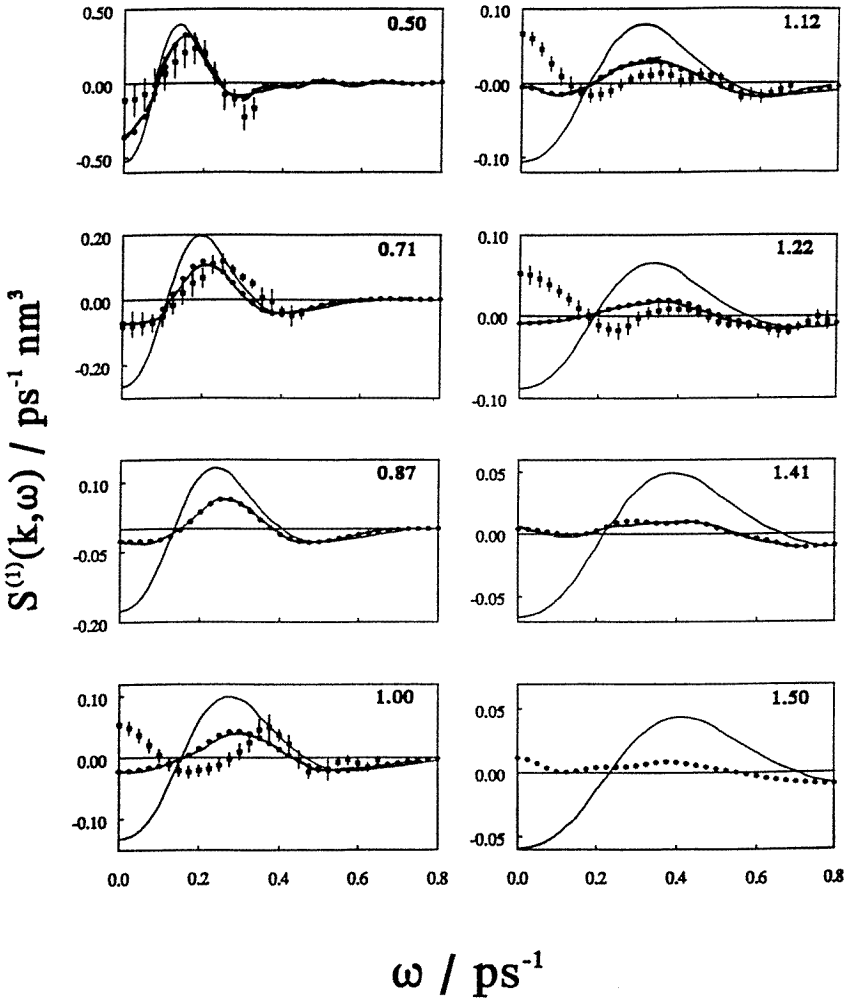

Figure 10. The experimental $S^{(1)}(k,\omega)$ for argon at room temperature (symbols with error bar), for MD calculations (dots) and for hard-sphere calculations (full line). The k values in nm^{-1} are given on the upper right-hand side of each plot.

an experiment has been performed in argon gas at room temperature, at low density and at low k values [23]. This experiment was realized by using the spectrometer IN5 with small-angle detection at the ILL, Grenoble. The low-k values were chosen because, given the density, the deviations are larger at smaller k. This can be understood simply by looking at the small-k behaviour of the $S(k)$.

The densities of the experiment were chosen such that $n\sigma^3 \ll 1$, while the k range was such that $0.3 < kl_0 < 5$. From the experimental density behaviour of $S(k,\omega)$ then $S^{(1)}(k,\omega)$ was obtained and compared with two theoretical predictions, the hard-sphere (HS) one [11] and a molecular dynamics calculation performed with a LJ potential [24]. Figure 10 gives this comparison and shows the clear disagreement with the HS prediction, with an increasing deviation as k increases, whereas the comparison with the LJ result is much better, albeit not satisfactory. This shows the importance of the true interaction potential in determining

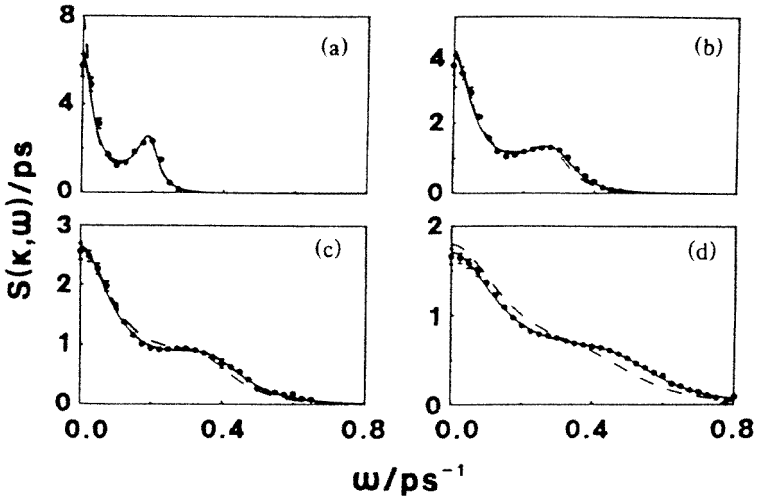

Figure 11. $S(k,\omega)$ at $n = 5.04$ nm^{-3}: experiments (dots with error bars), linearized hydrodynamics (broken line), three Lorentzians with fitted parameters (full line): (a) $k = 0.50$ nm^{-1}, (b) $k = 0.75$ nm^{-1}, (c) $k = 1.00$ nm^{-1} and (d) $k = 1.25$ nm^{-1}.

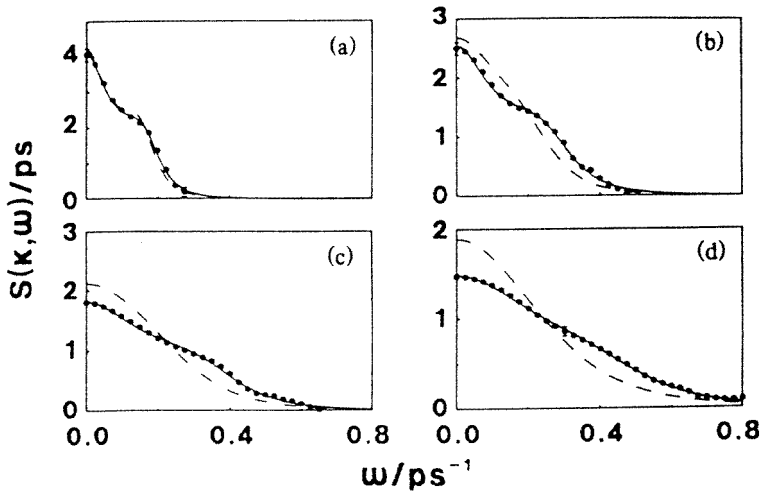

Figure 12. $S(k,\omega)$ at $n = 2.00$ nm^{-3}. Symbols and k values are as in figure 11.

the dynamics of the pair as should be expected, and the large sensitivity of $S^{(1)}(k,\omega)$ to the details of the pair interaction.

8. The small-angle $S(k,\omega)$ in moderately dense gases

For gas densities and k ranges within which $kl_0 < 1$ the transition from kinetic to hydrodynamic behaviour starts to show up in the fluid and collective excitations start to determine the shape of the $S(k,\omega)$. The experimental demonstration of this statement was possible with an experiment in argon at room temperature and at densities larger than those

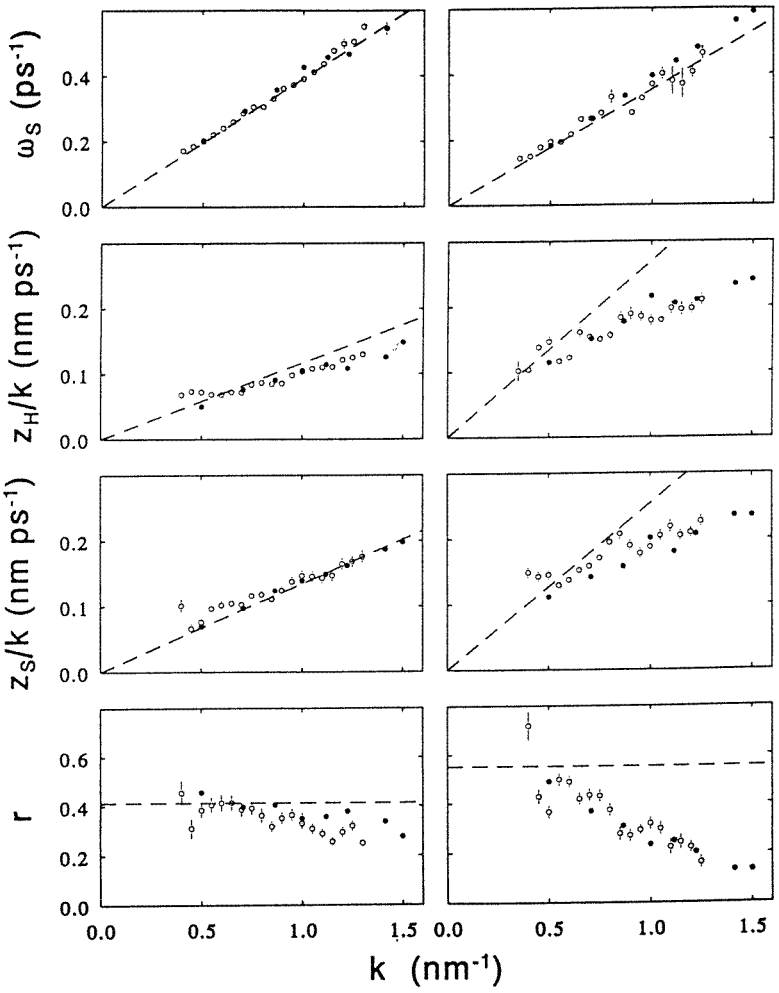

Figure 13. The four fitted parameters of the three-Lorentzian spectrum as functions of k at $n = 5.04$ nm^{-3} (left-hand side) and at $n = 2.00$ nm^{-3} (right-hand side). Experimental results (symbols with error bars), MD calculation with the LJ potential (dots) and linearized hydrodynamics (broken line).

in the previous case [25]. Also in this experiment the spectrometer IN5 with small-angle detection was used [24]. The experiment was performed at the two number densities 2.00 and 5.04 nm^{-3} which means $0.15 < kl_0 < 1.3$ for the k range presently used.

Figures 11 and 12 give the experimental $S(k, \omega)$ for the two densities at various k values compared to the three-Lorentzian equation, equation (23). Two cases are reported, one is for the spectrum (23) with the parameters given by the linearized hydrodynamics, the second is a simple least-squares fit of equation (23) with free parameters to the experimental data. From figure 12 it is clear that linearized hydrodynamics does not take account of the spectra at high k and at the lower density.

This is better seen in figure 13, in which the parameters of the fit to equation (23), namely ω_S, z_S, z_H and $r = A_S/A_0$ are given together with the predictions of hydrodynamics. In

figure 13 also the results of a molecular dynamics (MD) calculation of $S(k, \omega)$ for a LJ potential are given [26].

From figure 13 it is clear that departure from hydrodynamic behaviour towards kinetic behaviour has been demonstrated experimentally at the lower density and highest k values. This is confirmed also by the model MD calculation.

9. Conclusions

We have briefly recalled some of the results of a series of neutron scattering experiments in noble gases at various densities, both elastic and inelastic. From the comparison with available theories we can conclude the following.

(i) Precise low-density measurements of the static structure factor $S(k)$, in simple classical fluids, as a function of the density, can give experimentally determined pair potentials and information on the three-body contributions.

(ii) The study of the small-k dependence of the $c(k)$ allows one to determine the long-range potential, namely the London dispersion force, in atomic pairs as well as the asymptotic behaviour of the three-body corrections.

(iii) Comparison between experiments and theoretical calculations for high-density $S(k)$ in simple fluids shows that, depending on the thermodynamic state, approximately 95–98% of the total $S(k)$ can be ascribed to the pair potential interaction, if real potentials are used, and only a very small amount can be related to three-body effects, which show up better at low k values and intermediate densities. Also 85–90% of the pair contribution should be ascribed to the excluded volume effect, nevertheless 10–15% of the $S(k)$ in dense fluids is strictly related to the attractive part of the pair potential. Moreover, the density derivative of the $S(k)$, when available, is a quantity which is more suitable to study the connection with the form of the microscopic interaction.

(iv) The study of the density expansion of the $S(k, \omega)$ at low enough density permits one to derive the first dynamic correction to the free-gas behaviour in the $S(k, \omega)$ itself. This correction is related to the dynamic of the pair in the system and reflects the details of the real pair interaction potential.

(v) For sufficiently high densities neutron inelastic scattering at low k allows one to study the elementary excitations of the fluid in the hydrodynamic regime together with the transition from the hydrodynamic to the kinetic behaviour.

References

[1] Hansen J P and McDonald I R 1986 *Theory of Simple Liquids* (London: Academic)
[2] Egelstaff P A 1992 *An Introduction to the Liquid State* (Oxford: Clarendon)
[3] Aziz R A 1984 *Inert Gases* ed M L Klein (Berlin: Springer) p 5
[4] Reatto L and Tau M 1987 *J. Chem. Phys.* **86** 6474
[5] Teitsma A and Egelstaff P A 1980 *Phys. Rev.* A **21** 367
[6] Tau M, Reatto L, Magli R, Egelstaff P A and Barocchi F 1989 *J. Phys.: Condens. Matter* **1** 7131
[7] Reatto L and Tau M 1992 *J. Phys.: Condens. Matter* **4** 1
[8] Axilrod B M and Teller E 1943 *J. Chem. Phys.* **11** 299
[9] Casanova G, Dulla R J, Jonah D A, Rowlinson J S and Sanville G 1970 *Mol. Phys.* **18** 589
[10] Enderby J E, Gaskell T and March N H 1965 *Proc. Phys. Soc.* **85** 217
[11] Kamgar-Parsi B, Cohen E G D and de Schepper I M 1987 *Phys. Rev.* A **35** 4781
[12] Moraldi M, Celli M and Barocchi F 1989 *Phys. Rev.* A **40** 1116
[13] van Well A A and de Graaf L A 1985 *Phys. Rev.* A **32** 2396
[14] Fredrikze H, van Tricht J B, van Well A A, Magli R, Chieux P and Barocchi F 1989 *Phys. Rev. Lett.* **62** 2612

[15] Barker J A, Fisher R A and Watts R O 1971 *Mol. Phys.* **21** 657
[16] Magli R, Barocchi F, Chieux P and Fontana R 1996 *Phys. Rev. Lett.* **77** 846
[17] Kumar A and Meath W J 1985 *Mol. Phys.* **54** 823
[18] Barocchi F, Chieux P, Magli R, Reatto L and Tau M 1993 *Phys. Rev. Lett.* **70** 947
[19] Barocchi F, Chieux P, Magli R, Reatto L and Tau M 1993 *J. Phys.: Condens. Matter* **5** 4299
[20] Aziz R A and Slaman M J 1986 *Mol. Phys.* **58** 679
[21] Parola A and Reatto L 1995 *Adv. Phys.* **44** 211
[22] Barocchi F, Chieux P, Fontana R, Magli R, Meroni A, Parola A and Reatto L 1996 to be published
[23] Verkerk P, Bafile U, Barocchi F, de Graaf L A, Suck J B and Mutka H 1991 *Phys. Rev. Lett.* **67** 1262
[24] Bafile U, Barocchi F and Neumann M 1995 *Phys. Rev.* E **51** 3756
[25] Bafile U, Verkerk P, Barocchi F, de Graaf L A, Suck J B and Mutka H 1990 *Phys. Rev. Lett.* **65** 2394
[26] Bafile U, Barocchi F, Neumann M and Verkerk P 1994 *J. Phys.: Condens. Matter* **6** A107